JOURNAL OF APPLIED ELECTROCHEMISTRY 22 (1992) 464–470

X-ray diffraction and thermal wave analysis of primary recrystallization in electrodeposited copper layers at room temperature

S. SURNEV

Department of Solid State Physics, Faculty of Physics, Sofia University, 5A. Ivanov blvd, Sofia 1126, Bulgaria

I. TOMOV

Institute of Physical Chemistry, Bulgarian Academy of Sciences, Sofia 1040, Bulgaria

Received 21 February 1991; revised 28 August 1991

An X-ray diffraction and thermal wave study of the microstructural and thermal parameters of electrodeposited copper layers was carried out. The effect of the deposition temperature on the growth and recrystallization textures as well as on the thermal diffusivity (resistivity) of copper layers was investigated. The kinetics of primary recrystallization and of stored energy release has been estimated from the orientation density and thermal resistivity data, respectively. The behaviour of the kinetic curves is discussed in relation to the heterogeneous stored energy distribution in the material.

1. Introduction

During metal electrodeposition a large number of imperfections form, causing an increase in the internal energy. This increment, or the so-called stored energy [1], provides the driving force for recovery and recrystallization.

Recovery processes in electrodeposited copper have been studied by X-ray diffraction (XRD) both after annealing [2–4] and at room temperature [5]. Earlier papers [2, 6] report on thermally activated recrystallization in thin copper layers. It was shown in previous studies [7, 8] that recovery and recrystallization in electrodeposited copper layers proceed at an observable rate even at room temperature. As a result there were changes in the structure and microhardness. In a recent paper [9] the effect of the cathode current density, D_c, on both the growth texture and the rate of release of stored energy was investigated. This rate was estimated from the rate of decrease of the pure integral breadth of the respective XRD lines.

Additional information on such recovery processes in metal electrodeposits may be obtained from the kinetic study of texture evolution and of the stored energy release. With the help of XRD only a small fraction of the total stored energy may be determined, this is the elastic stored energy, V_{el}. This is linked mainly with the tension fields around dislocations in the bulk of crystallites. The other, dominating, part is the stored energy of grain boundaries, V_{gb}. The release of V_{gb} is associated with the reduction of dislocation density in the grain boundary region. The kinetics of V_{gb} release may be determined using the kinetics of such material property, which is sensitive to the structure of grain boundaries. As was shown by Gangulee [3] the electrical resistivity, ρ_e, of electroplated copper films is much higher than that of bulk copper. The excess resistivity has been attributed to dislocations, grain boundaries and twins.

The thermal resistivity, W, can also be used to characterize the defect structure of the electroplated films, since it is related to the electrical resistivity through the Widemann-Franz law [10]:

$$W = \frac{\rho_e}{L_0 T} \quad (1)$$

where L_0 is the Lorenz ratio and T is the absolute temperature.

In the present paper the influence of the deposition temperature on both the growth texture and the thermal properties of electrodeposited copper layers is studied. The kinetics of stored energy release in relation to the textural evolution during the recrystallization at room temperature is also examined. Particular attention is paid to the use of two independent approaches, i.e. X-ray diffraction and thermal wave measurements, which lead to complementary results.

2. Experimental details

2.1. *Specimen preparation*

The specimens were electrodeposited copper layers. Their deposition was carried out on rotating disc electrodes of two types. Brass electrodes, with a diameter of 32 mm, were used for the X-ray diffraction measurements and iron electrodes, with a diameter of 9 mm, were used for the thermal wave measurements. The layers were plated in the electrolyte proposed in [11] with the following composition: $CuSO_4 \cdot 5H_2O$ 220 g dm^{-3}, H_2SO_4 30 g dm^{-3}, NaCl 50 g dm^{-3} and brightener agents THB-I and THB-II 3 cm^3 dm^{-3}. Specimens A, B and C were deposited at cathode

0021-891X/92

current density $D_c = 8\,A\,dm^{-2}$ and at deposition temperatures, T_0, of 22, 30 and 35° C, respectively. The thickness of all specimens was $\sim 70\,\mu m$. As standards for X-ray analysis specimens prepared at the same conditions and annealed for 1 h in vacuum at 500° C were employed.

2.2. *X-ray diffraction analysis*

The X-ray diffraction measurements of the pole figures were carried out with a texture goniometer, reflection scheme [12], CuK_α radiation. The X-ray diffraction line profile was measured by continuous scan with an X-ray diffractometer (Philips, CuK_α radiation, isolated with a LiF focusing monochromator). The scan speed was $0.5°\,min^{-1}$ in the 2θ scale.

The orientation density gives the frequency with which the fibre axis lies in different crystal directions. By means of diffractometric measurements this density may be determined only in the low indexed crystal directions, in which it is equivalent to the pole density [13]. The orientation density P_{hkl} was calculated in a manner, described in [9].

The effective crystallite size, D, and the strains, $\tilde{e}$, were determined from the X-ray diffraction line broadening analysis of a single line [14]. α_2 elimination was carried out by the Rachinger method [15]. The elastic stored energy was assessed by the Faulkner formula [16]:

$$V_{el} = \frac{15E_{hkl}}{2(3 - 4\nu + 8\nu^2)}\tilde{e}^2 \qquad (2)$$

where E_{hkl} is Young's modulus in the $\langle h\,k\,l\rangle$ direction and ν is Poisson's ratio. The stored energy of grain boundaries is estimated from the expression derived in [17]:

$$V_{gb} = K\sigma v/D \qquad (3)$$

where K is a constant between 1 and 3, σ is the average specific grain boundary energy, v is the molar volume of the metal and D is the average grain size. For copper $\sigma = 645 \times 10^{-7}\,J\,cm^{-2}$, $v = 7\,cm^3\,mol^{-1}$ and $K = 2$ is taken [17].

2.3. *Thermal wave analysis*

Thermal wave (TW) techniques are particularly well suited for non-destructive characterization of thermal properties of thin films [18]. In most cases the thermal wave is produced by modulated laser beam, aimed at the surface of a sample under test. The TW will propagate through the film–substrate interface. The resulting surface temperature can be measured in several ways. In our case we utilize the method of optical beam deflection (OBD), also known as "mirage" effect [19]. This method uses the deflection of a probe laser beam that skims at the sample surface to register the temperature variations. The experimental setup is shown in Fig. 1. The pumped Ar laser beam ($\lambda = 514.5\,nm$), of power 1 W, falls unfocused (spot size $\sim 3\,mm$) at normal incidence on the sample surface. This beam is modulated by a mechanical chopper at frequencies varying from 100 Hz to 2.5 kHz. The periodical deflection of the probe He–Ne laser beam ($\lambda = 632.8\,nm$), of power 0.5 mW, is detected by a position sensitive detector (SIEMENS-type BPX 48). The signal from the detector (mirage signal) is fed to a PARC 5301 vector lock-in amplifier, connected to a PC through a serial interface RS232C.

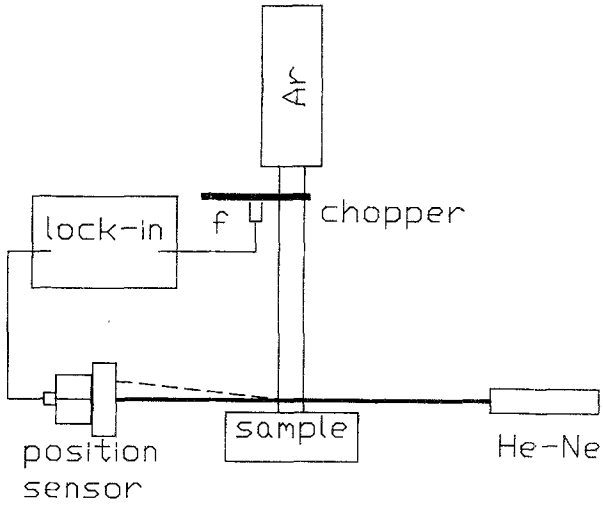

Fig. 1. Schematic diagram of the "mirage" effect setup.

The quantity measured by the TW method is the thermal diffusivity α. The thermal resistivity is related to α through:

$$W = \frac{1}{\alpha\rho C} \qquad (4)$$

where ρ and C are the density and the specific heat, respectively. The method for determining the thermal diffusivity, α, of electrodeposited copper layers is described in detail in [20]. It consists in the measurement of the phase difference, $\Delta\phi$, between two mirage signals, one from the film-substrate specimen and the other from the substrate, as a function of the modulation frequency, f. According to [20] $\Delta\phi$ is given by

$$\Delta\phi = \tan^{-1}\left[\frac{2R_{sb}\sin(2x)}{\exp(2x) - R_{sb}^2\exp(-2x)}\right] \qquad (5)$$

where $x = (\pi f/f_c)^{1/2}$, $f_c = \alpha l^{-2}$ is the so-called characteristic frequency of the film of thicknes l and R_{sb} is called the thermal reflection coefficient at the film–substrate interface. By fitting the experimental data to Equation 5 by the method of least squares, the parameters R_{sb} and f_c (and hence α) can be determined.

In connection with the study of recrystallization in copper electrodeposits at room temperature it is necessary to estimate to what extent the laser heating may disturb this process. The dc surface temperature rise in the centre of the laser beam spot can be calculated from the expression, derived in [21]:

$$\Delta T = \frac{P_0(1 - r)}{2\sqrt{\pi a\kappa}} \qquad (6)$$

where P_0 is the laser beam power, a is the laser beam radius, κ is the thermal conductivity and r is the optical reflection coefficient of the sample. Taking

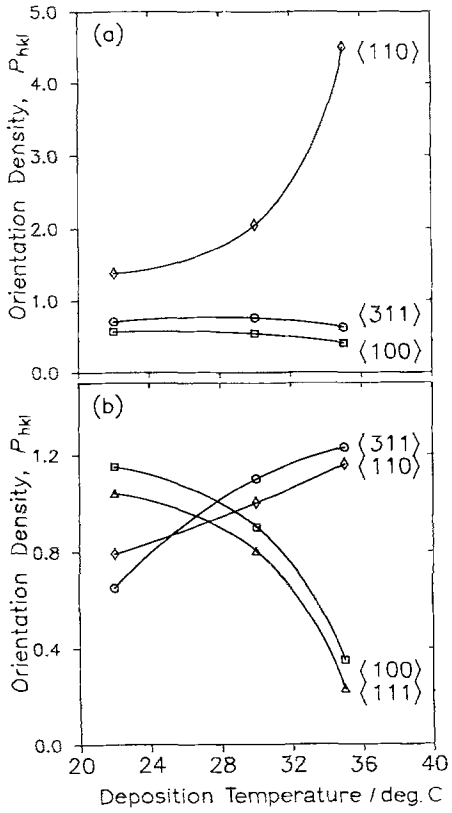

Fig. 2. Plot of the orientation densities, P_{hkl}, of the growth texture (a) and the recrystallization texture (b) against the deposition temperature T_0.

$P_0 = 1\,W$ and $a = 1.5 \times 10^{-3}\,m$ and using handbook data for copper [22] $r = 62\%$ and $\kappa = 400\,W\,m\,K^{-1}$ $\Delta T \simeq 0.2°C$, which is within the limits of the mean 24 h temperature variation.

3. Results

The study of recrystallization in electrodeposited copper layers was carried out at room temperature.

3.1. *Texture*

The electrodeposited copper layers have a fibre texture. According to the pole figure data the as-fabricated growth texture of the A, B and C specimens consists of a single component with ⟨1 1 0⟩ orientation. The texture was monitored quantitatively be determining the orientation density, P_{hkl}, in relevant ⟨h k l⟩ directions. Figure 2 shows the orientation densities P_{hkl} in the ⟨1 0 0⟩, ⟨1 1 0⟩, ⟨1 1 1⟩ and ⟨3 1 1⟩ directions for the growth texture (Fig. 2a) and for the recrystallization texture (Fig. 2b) of A, B and C (i.e. as a function of temperature of deposition T_0). It is seen from Fig. 2a that the increase in T_0 causes a marked increase in the sharpness of the main component ⟨1 1 0⟩ and a slight decrease in P_{100} and P_{311} (P_{111}, which is not shown in Fig. 2a, is identical with P_{100}) of the growth texture (GT). The recrystallization texture (RT) of specimen A, from the pole figures data, consists of ⟨1 0 0⟩ + ⟨2 2 1⟩ + ⟨1 1 1⟩ components (⟨2 2 1⟩ is a twin component of the ⟨1 0 0⟩ recrystallization component). At higher deposition temperatures (specimens B and C) P_{311} increases, while P_{100} and P_{111} decrease.

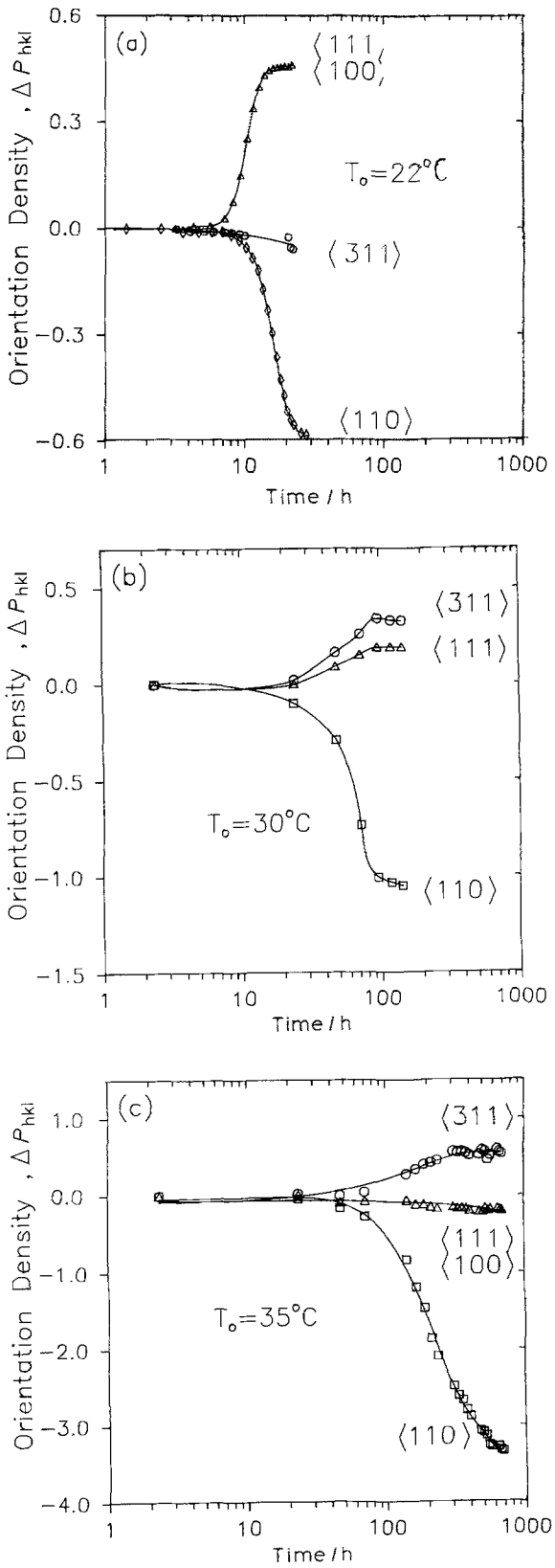

Fig. 3. Plots of the orientation densities, ΔP_{hkl}, against time: (a) specimen A, (b) specimen B and (c) specimen C.

To present the changes of the orientation density, P_{hkl}, against time for specimens A, B and C the orientation density change in relation to their value $P_{hkl}(0)$ in the as-fabricated state is used [9]:

$$\Delta P_{hkl} = P_{hkl}(t) - P_{hkl}(0) \qquad (7)$$

Figures 3a, b, and c show ΔP_{hkl} against time for the

Table 1. Effective crystallite size, D, strains, $\tilde{e}$, elastic stored energy, V_{el}, and stored energy of the grain boundaries, V_{gb}

Specimen	*D*/nm	$\tilde{e} \times 10^3$	V_{el}/J mol^{-1}	V_{gb}/J mol^{-1}	V_{el}/V_{gb}/%
A	71.4 ± 5	1.2 ± 0.1	7.5 ± 0.8	125 ± 8	6 ± 1
B	128.9 ± 8	1.3 ± 0.1	7.9 ± 0.8	67 ± 5	11 ± 2
C	218.5 ± 10	0.8 ± 0.1	5.0 ± 0.8	37 ± 5	13 ± 2

specimens A, B and C, respectively. It is evident that the lower the deposition temperature, the higher the rate of texture change. The primary recrystallization can be considered finished in specimen A 24 h after deposition while in specimen C it is prolonged 30 days.

3.2. *Effective crystallite size, strains and stored energy*

The effective crystallite size and strains were determined from the broadening analysis of XRD line 2 2 0, where the crystallites of the main texture component ⟨1 1 0⟩ reflect. Table 1 lists the results for the effective crystallite size, D, the strains, $\tilde{e}$, the elastic stored energy, V_{el}, and the stored energy of grain boundaries, V_{gb}, determined in the as-fabricated state. These results indicate that with increase in deposition temperature the effective crystallite size increases (V_{gb} decreases). The value of D for the specimen C lies outside the range of reliable determination ($D \leqslant 150$ nm). The strains are the lowest in specimen C while they are higher and approximately equal (within the error limits) in specimens A and B.

3.3. *Thermal diffusivity and thermal resistivity*

Figure 4 is a plot of the phase difference $\Delta\phi$ against square root of the modulation frequency for sample A, measured 4 h (curve 1) and 36 h (curve 2) after the deposition. A least squares fitting program yielded the values for f_c and R_{sb}. From f_c and 1 ($l = 70\,\mu$m) the thermal diffusivity, α, was computed. These parameters are as follows: curve 1: $f_c = 17.1 \pm 0.5$ kHz; $R_{sb} = 0.48 \pm 0.02$ and $\alpha = 0.83 \pm 0.03\,\text{cm}^2\text{s}^{-1}$; curve 2: $f_c = 22.5 \pm 0.5$ kHz; $R_{sb} = 0.58 \pm 0.02$ and $\alpha = 1.10 \pm 0.03\,\text{cm}^2\text{s}^{-1}$.

Figure 5 shows the thermal diffusivity of electrodeposited copper layers as a function of the deposition temperature. Curve 1 refers to the values of α, measured in the as-fabricated state, while curve 2 refers to the relevant values in the recrystallized state. It appears that the thermal diffusivity in the recrystallized state, α_0, does not depend on T_0 and is close to the nominal value for copper, i.e. $1.12\,\text{cm}^2\text{s}^{-1}$ [22]. The thermal diffusivity in the as-plated state (curve 1) is lower than α_0 and decreases with decrease in T_0.

The dimensionless quantity $\Delta W/W_0$ may be introduced. Here W_0 is the sample thermal resistivity in the recrystallized state. $\Delta W = W - W_0$ is the thermal resistivity increment, which is due to the various electron scattering mechanisms. Using Equations 4,

$$\Delta W/W_0 = \alpha_0/\alpha - 1 \qquad (8)$$

Figure 6 shows $\Delta W/W_0$ against time for the specimens A, B and C. The change of $\Delta W/W_0$ against time proceeds at maximum rate in specimen A and at minimum rate in C.

4. Discussion

4.1. *Recrystallization kinetics determined from the texture data*

The texture of an electrodeposited metal is controlled by several variables, such as the substrate structure, cathode current density, deposition temperature and

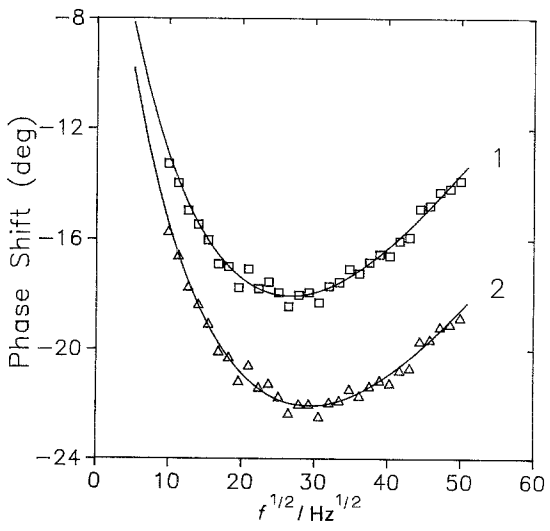

Fig. 4. Plot of the phase difference $\Delta\phi$ against the square root of the modulation frequency, measured at 4 h (curve 1) and 36 h (curve 2) after the deposition of specimen A. These curves are fitted by the least squares method (solid lines).

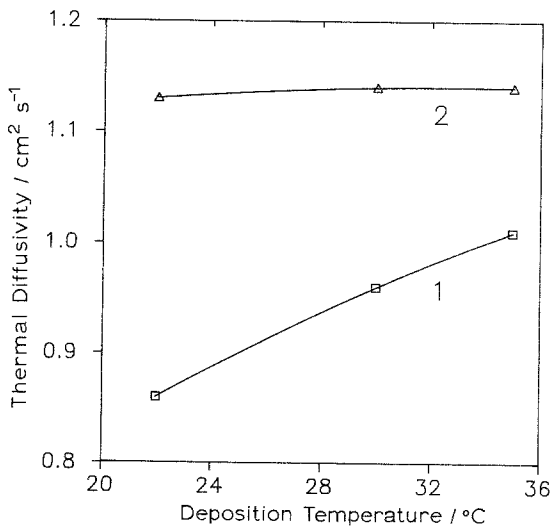

Fig. 5. Thermal diffusivity of electrodeposited copper layers, measured as a function of the deposition temperature. Curve 1 refers to the as-fabricated state and curve 2 refers to the recrystallized state.

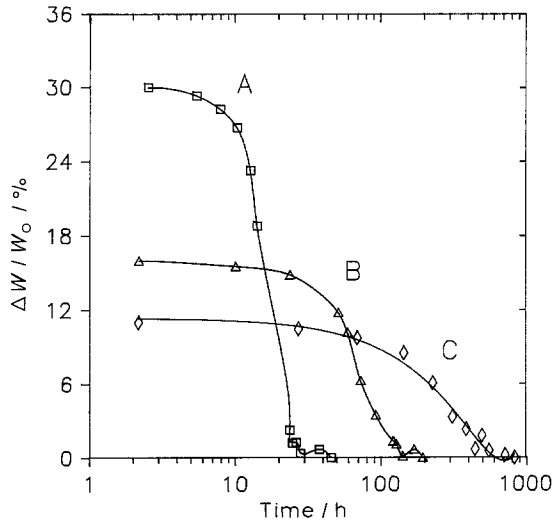

Fig. 6. Plot of the thermal resistivity increment, $\Delta W/W_0$, against time for specimens A, B and C.

so on. In the present work the deposition temperature was varied and the other deposition parameters were kept constant. The influence of the temperature of deposition may be considered in two directions: (i) on the growth and recrystallization textures and (ii) on the rate of texture changes.

Usually increase in T_0 acts in the same way as decrease in cathode current density, D_c [23]. The increase of the orientation density of the GT component $\langle 1\,1\,0\rangle$ at higher T_0 (Fig. 2) is analogous to the increase of P_{110} with decrease of D_c, observed in [9]. Such a relation holds for P_{100} and P_{111}, which decrease with increase in T_0. Since the recrystallization texture is determined from the growth texture, T_0 and D_c have similar effect on the *RT*.

The texture changes, shown in Fig. 3, are due to the primary recrystallization alone. This allows information for the recrystallization kinetics in copper electrodeposits at room temperature to be obtained. The kinetics of isothermal recrystallization are described by the classic Johnson-Mehl-Avrami (JMA) equation [24, 25]:

$$X = 1 - \exp\left[-0.693(t/t_{0.5})^k\right] \qquad (9)$$

where X is the fraction of the recrystallized material at time t, $t_{0.5}$ is the time for 50% recrystallization and is related to the speed with which recrystallization proceeds. The exponent k, which describes the shape of X-t curve, is determined from the time dependence rate of nucleation and growth and the dimensionality of the growth fronts.

The recrystallized fraction, X, can be estimated from the orientation density data in a way proposed by Gangulee [4]:

$$X = \frac{P^0_{hkl} - P_{hkl}(t)}{P^0_{hkl} - P_{hkl}(0)} \qquad (10)$$

Here P^0_{hkl} is the orientation density value, measured in the recrystallized state. The assessment of X was performed in the $\langle 1\,1\,0\rangle$ direction since the evolution of P_{110} gives the most complete picture of the recrystallization kinetics in the samples. This is due to the fact

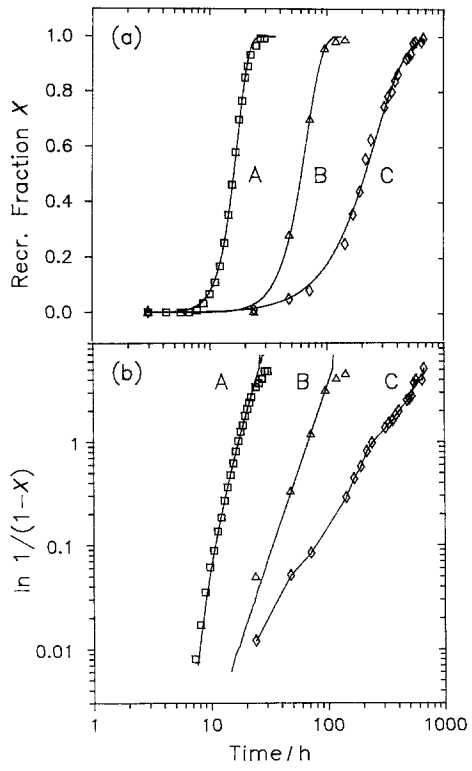

Fig. 7. (a) Plot of the recrystallized fraction, X, against time for specimens A, B and C; (b) Plot of log [ln $(1 - X)$] against time (JMA plot) for specimens A, B and C.

that the growth texture has one component, $\langle 1\,1\,0\rangle$, and the recrystallization in other crystal directions is accomplished at the expense of consuming the $\langle 1\,1\,0\rangle$ component of the GT. Replacing P_{110} in Equation 10 we obtain the fraction X', which has not been recrystallized at the moment t. For the recrystallization fraction X it follows that: $X = 1 - X'$. Figure 7a represents a plot of X as a function of time for samples A, B and C. These curves show the sigmoidal shape typical of the kinetics of primary recrystallization. The solid lines represent the theoretical curves, fitted according to Equation 10 with the values of $t_{0.5}$ and k, given in Table 2 (XRD section). By analogy with [9] the quantity R, equal to the reciprocal value of $t_{0.5}$, which has a meaning of a *recrystallization rate* is defined. R is higher for specimen A where the growth texture is weaker (Fig. 2a) and the crystallite size is smaller than in the other two samples. This may be explained by the sub-grain coalescence model, proposed by Hu [26]. According to this model the recrystallization tendency is stronger in deformed crystals with weak deformation (growth) textures and with small sub-grain size.

Table 2. Kinetic parameters $t_{0.5}$ and k, determined from X-ray diffraction (XRD) and thermal wave (TW) analysis, respectively

	XRD		*TW*	
Specimen	$t_{0.5}/h$	k	$t_{0.5}/h$	k
A	16.1 ± 0.2	4.6 ± 0.1	20.1 ± 0.4	3.5 ± 0.3
B	60.7 ± 0.5	3.3 ± 0.3	70.2 ± 0.8	2.5 ± 0.4
C	213.0 ± 3.0	1.7 ± 0.2	227.0 ± 3.0	1.4 ± 0.4

It is seen from the XRD data, presented in Table 2, that the exponent k is maximum for specimen A and minimum for specimen C. The behaviour of curves in Fig. 7b, which is the so-called JMA plot of Fig. 7a, reveals some features of the recrystallization process in electrodeposited copper layers. It is evident that the slopes of the JMA curves give the value of k. At $X > 0.8$ in Fig. 7b deviation from linearity is observed for samples A and B. This deviation has been characterized by Vandermeer and Gordon [17] as "retardation" of recrystallization. This retardation was thought to be due to competing recovery during the course of recrystallization, which reduces the driving force for recrystallization. This means that the retardation effect is more pronounced at higher values of the ratio V_{el}/V_{gb}, as confirmed by Table 1. The calculations of Rollett [27] indicate that the model of Vandermeer and Gordon could not explain the low JMA exponent obtained for sample C and for many other cases cited in the review of Doherty [28]. The JMA curve of specimen C has a complex shape and may be considered as composed of several JMA curves, each with its own slope. Such a structure has been observed by Luton *et al.* [29] for recrystallization after hot working of copper. The results of the statistical model, proposed in [28], show that the complex shape of the JMA curve and the low exponents should be obtained if non-random distribution of nucleation sites is suggested. The case with specimen C can be explained on this basis. Due to the higher deposition temperature ($T_0 = 35°$ C) it is most likely that a part of the recrystallization nuclei have been formed during the deposition process. After the deposition, the copper layer is held at room temperature at which the recrystallization proceeds at slower rate. For the onset of recrystallization at this temperature much activation energy or time (incubation period) is required. By this reason in some parts of the material (with lower stored energy) the recrystallization has started while in others (with higher stored energy) it has not yet. This grain to grain variation of the stored energy seems to lead to the anomalous shape of curve C as well as to the value of JMA exponent, which is much less than that theoretically predicted.

4.2. *Stored energy release kinetics, revealed by thermal wave analysis*

The use of the thermal resistivity, W, instead of the thermal diffusivity, α, is due to the fact that W, as ρ_e, may be expressed as a sum of resistivities of individual scattering mechanisms. As shown in [3] the electrical resistivity increment $\Delta\rho_e$ at room temperature is mainly due to the grain boundaries. From the Widemann–Franz law (Equation 1) it follows that this would also be valid for the thermal resistivity increment ΔW. This means that ΔW is related to the average grain size $\langle D\rangle$. A simple assessment of this connection can be derived, taking into account that $\Delta W \approx \Delta W_{gb} = W_s\langle S\rangle/\langle V\rangle$, where W_s is the specific grain boundary thermal resistivity and $\langle S\rangle$ and $\langle V\rangle$ are the average surface and volume per grain, respectively. Assuming spherical grains we obtain:

$$\Delta W/W_0 = \text{const}/\langle D\rangle \qquad (11)$$

For fine-grained specimens in the as-fabricated state it is considered that $\langle D\rangle \approx D_{110}$. Figure 8 is a plot of $\Delta W/W_0$ against $1/D_{110}$, measured in the as-fabricated state. As seen from the figure the three points (for each sample) lie very close to the straight line, passing near the point (0, 0). This fact confirms the validity of Equation 11. From Equations 3 and 11 it follows that the stored energy of grain boundaries, V_{gb}, is proportional to $\Delta W/W_0$. This makes it possible to obtain information on the kinetics of stored energy release. Such information could not be derived from the kinetics of the effective crystallite size because of the restricted validity of XRD method at higher D.

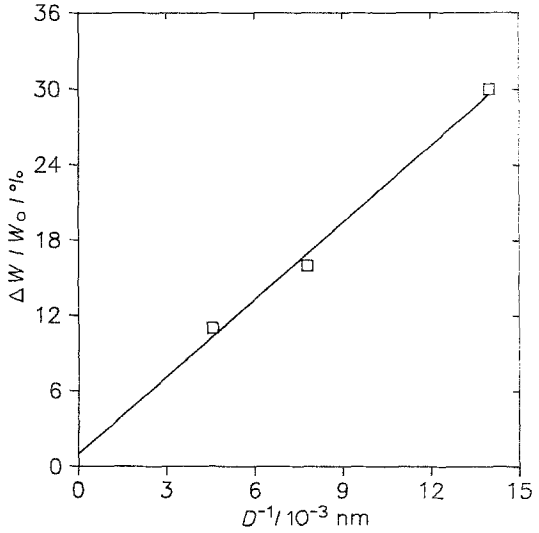

Fig. 8. Thermal resistivity increment, $\Delta W/W_0$, as a function of the reciprocal crystallite size, $1/D_{110}$, measured in the as-plated state.

Let Y denote the fraction of V_{gb} liberated at time t. From the proportionality of V_{gb} and $\Delta W/W_0$ it follows that

$$Y = 1 - [\Delta W/W_0]/[\Delta W(0)/W_0] \qquad (12)$$

where $\Delta W(0)$ is the excess resistivity, measured in the as-fabricated state. Figure 9 shows Y as a function of t for specimens A, B and C. As demonstrated in [1] the kinetics of stored energy release should obey the JMA equation (9). The solid lines represent the theoretical curves, calculated from Equation 9 with the results of least squares fit of experimental curves. These results are listed in Table 2 (TW section). There is a correspondence in TW parameters with those obtained by the XRD analysis.

5. Conclusions

The effect of the deposition temperature on the structure and the thermal properties of electrodeposited copper layers has been studied. The kinetics of primary recrystallization and stored energy release in these layers at room temperature, has been estimated from the orientation density and thermal resistivity data, respectively. It has been established that: (i) specimens

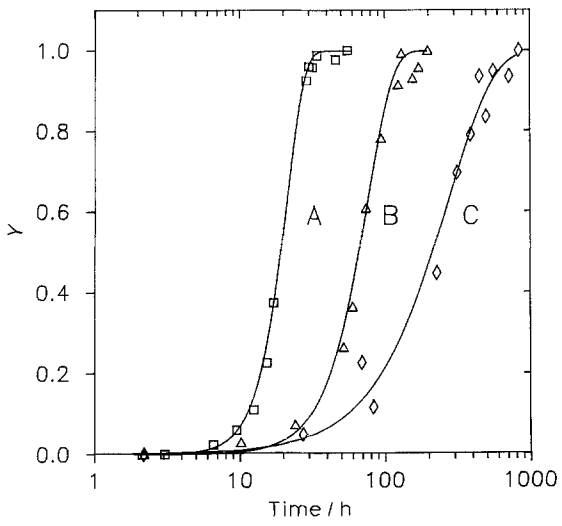

Fig. 9. Plot of the fraction of stored energy release against time for specimens A, B and C.

prepared at lower deposition temperature have lower sharpness of the main component of the growth texture ⟨1 1 0⟩, higher strain, lower crystal size and lower thermal diffusivity; (ii) the recrystallization rate is lower for specimens prepared at higher T_0; (iii) the anomalous shape of the JMA curve and the lower value of the JMA exponent for the specimen, prepared at higher T_0 is due to grain variation of the stored energy.

References

[1] M. B. Bever, D. L. Holt and A. L. Titchener, *in* 'Progress in Materials Science' (edited by B. Chalmers, J. W. Christian and T. B. Massalski) vol. 17, Pergamon Press, Oxford (1973).
[2] E. M. Hofer and H. E. Hintermann, *J. Electrochem. Soc.* **112** (1965) 167.
[3] A. Gangulee, *J. Appl. Phys.* **43** (1972) 867.
[4] *Idem, ibid.* **43** (1972) 3943.
[5] Yu. M. Polukarov, Ju. D. Gamburg, M. I. Tcherepenina, *in* 'Issledovania po electroosajdeniu i rastvoreniu metallov', Nauka, Moskow (1971) pp. 146–52.
[6] A. Gangulee, *J. Appl. Phys.* **45** (1974) 3749.
[7] D. S. Stoychev, I. V. Tomov, I. B. Vitanova, *J. Appl. Electrochem.* **15** (1985) 879.
[8] I. V. Tomov, D. S. Stoychev, I. B. Vitanova, *Ibid.* **15** (1985) 887.
[9] Sv. Surnev, I. Tomov, *J. Appl. Electrochem.* **19** (1989) 752.
[10] R. Berman, *in* 'Thermal Conduction in Solids', Clarendon Press, Oxford (1976).
[11] D. Stoychev, I. Vitanova, I. Pojarliev and S. Rashkov, *Poligraphia (Russ.)* **9** (1984) 37.
[12] L. G. Schulz, *J. Appl. Phys.* **20** (1949) 1033.
[13] H.-J. Bunge, *in* 'Texture Analysis in Materials Science – Mathematical Methods', Butterworths, London (1982) p. 127.
[14] R. Delhez, Th. H. de Keijser and E. J. Mittemeijer, *Fres. Z. Anal. Chem.* **312** (1982) 1.
[15] W. A. Rachinher, *J. Sci. Instrum.* **25** (1948) 254.
[16] E. A. Faulkner, *Phil. Mag.* **5** (1960).
[17] R. A. Vandermeer and P. Gordon, *in* 'Recovery and recrystallization of metals' (edited by L. Himmel), Gordon and Breach, New York (1963) pp. 221–59.
[18] A. Rosencwaig and A. Gersho, *J. Appl. Phys.* **47** (1976) 64.
[19] A. C Boccara, D. Fournier and J. Badoz, *ibid.* **36** (1980) 136.
[20] J. P. Roger, F. Lepuotre, D. Fournier and A. C. Boccara, *Thin Solid Films* **155** (1987) 165.
[21] S. Surnev and D. Ivanov, *Revue Phys. Appl.* **25** (1990) 457.
[22] American Institute of Physics 'Handbook', 3rd ed. (edited by D. E. Gray), McGraw-Hill, New York (1972).
[23] G. I. Finch, A. Willman and L. Yang, *Disc. Faraday Soc.* **1** (1947) 144.
[24] W. A. Johnson and R. F. Mehl, *Trans. AIME* **135** (1939) 416.
[25] M. Avrami, *J. Chem. Phys.* **7** (1939) 1103; *J. Chem. Phys.* **8** (1940) 212; *J. Chem. Phys.* **9** (1941) 177.
[26] H. Hu, *in* 'Recovery and recrystallization of metals' (edited by L. Himmel), Gordon and Breach, New York (1963) pp. 311–378.
[27] A. D. Rollett, M. S. Thesis, Drexel University (1986).
[28] R. D. Doherty, A. R. Rollet and D. J. Srolovitz, *in* Proc. 7th Risø Int. Symp. on Metallurgy and Mater. Sci. (1986) pp. 53–67.
[29] M. J. Luton, R. A. Petovik and J. Jonas, *Acta Metall.* **28** (1980) 729.